Dynamics of unidirectional phonon-assisted transport of photoexcited carriers in step-graded In-x(Al0.17Ga0.83)(1-x)As/Al0.17Ga0.83As multiple quantum wells

Machida, S.; Matsuo, M.; Fujiwara, K.; Folkenberg, J.R.; Hvam, Jørn Märcher

Published in:
Physical Review B Condensed Matter

Link to article, DOI:
10.1103/PhysRevB.67.205322

Publication date:
2003

Document Version
Publisher's PDF, also known as Version of record

Dynamics of unidirectional phonon-assisted transport of photoexcited carriers in step-graded $In_x(Al_{0.17}Ga_{0.83})_{1-x}As/Al_{0.17}Ga_{0.83}As$ multiple quantum wells

S. Machida, M. Matsuo, and K. Fujiwara*
Kyushu Institute of Technology, Tobata, Kitakyushu 804-8550, Japan

J. R. Folkenberg
Crystal Fibre A/S, Blokken 84, DK-3460 Birkerød, Denmark

J. M. Hvam
Research Center COM, Technical University of Denmark, Building 349, DK-2800 Kgs. Lyngby, Denmark
(Received 8 October 2002; revised manuscript received 19 February 2003; published 27 May 2003)

The dynamics of perpendicular transport of photoexcited carriers assisted by phonon scattering is investigated in a novel step-graded $In_x(Al_{0.17}Ga_{0.83})_{1-x}As$ quantum-well heterostructure by measuring the temperature dependence of spectrally and temporally resolved photoluminescence (PL). When builtin potential gradients are present in the quantum-well heterostructure due to variations in the In mole fraction (x) in the well, carriers that are thermally released by the particular well move unidirectionally from shallower to deeper wells. That is, asymmetric unidirectional motion of photoexcited carriers is possible via phonon-assisted activation above the barrier band-edge state. We have directly measured this perpendicular motion of photoexcited carriers by monitoring the transient PL signals from the different wells, which are spectrally separated. A rate equation analysis rigorously explains the dynamical changes of the PL signal intensities from the quantum wells as a function of lattice temperature. Our study of PL dynamics proves the asymmetric perpendicular flow of photoexcited carriers and the capture by the deeper quantum wells, providing firm evidence for the dynamical carrier flow and capture processes in the novel heterostructure.

DOI: 10.1103/PhysRevB.67.205322 PACS number(s): 78.66.Fd, 78.47.+p, 78.55.Cr, 73.63.Hs

I. INTRODUCTION

In semiconductor quantum heterostructures, a variety of interesting perpendicular transport processes have been reported such as Fowler-Nordheim tunneling,[1] tunneling-assisted hopping conduction,[2] sequential resonant tunneling,[3,4] and Bloch-type transport via extended miniband states,[5,6] which are all based on tunneling phenomena.[7] When carriers are placed in a heterostructure with builtin potential gradients, however, they can undergo perpendicular motion or inversely be blocked from motion for enhancing stimulated emission.[8] By designing the more refined heterostructures utilizing modern growth technology,[9] tunneling-assisted interwell transitions and intersubband transitions are applied for unipolar quantum cascade lasers[10] and highly sensitive photodetectors.[11] Therefore, the understanding of cascading flow and/or capture of injected or photoexcited carriers in such composite quantum-well (QW) heterostructures is crucial for device applications. However, most of the previous studies discussing the mechanisms of capture and relaxation processes are concerned with the perpendicular transport of photoexcited carriers in monoperiodic systems such as semiconductor superlattices.[3,5,12] Only a few reports[13,14] have been presented for composite heterostructures comprising a number of dissimilar quantum wells. In this paper, perpendicular motion of photoexcited electron and hole pairs assisted by phonon scattering is investigated in a novel step-graded staircase heterostructure consisting of five-step strained $In_x(Al_{0.17}Ga_{0.83})_{1-x}As$ multiple quantum wells by time-resolved photoluminescence (PL) experiments. PL spectra of the sample reveal five distinct peaks corresponding to the QW layers, which dramatically evolve with increasing lattice temperature. We find that, as temperature increases, some of the PL peaks first increase their relative intensities in the intermediate temperature range and then decrease the signal amplitudes progressively from shorter-wavelength sides. These changes of the PL intensities as a function of temperature reflect the fact that the photoexcited carriers move unidirectionally from shallower to deeper QW's via phonon-assisted activation above the barrier band-edge state. This unidirectional phonon-assisted transport is realized between a shallow and a deep QW, as schematically illustrated in Fig. 1. Without the neighboring deeper well, the

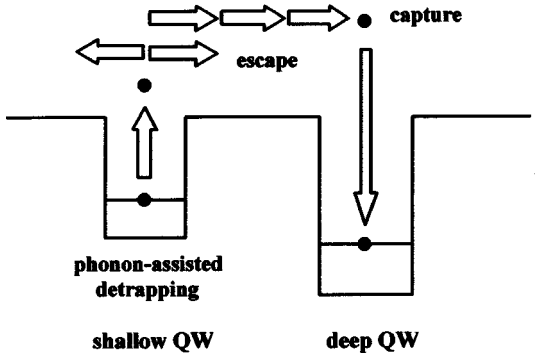

FIG. 1. Concept of unidirectional phonon-assisted motion of carriers towards the lower potential side due to asymmetry of the built-in potential profile. Note that, when the neighboring deeper well exists, the carriers escaping from the shallower well are captured by that deeper well, resulting in the asymmetric transport along the growth direction.

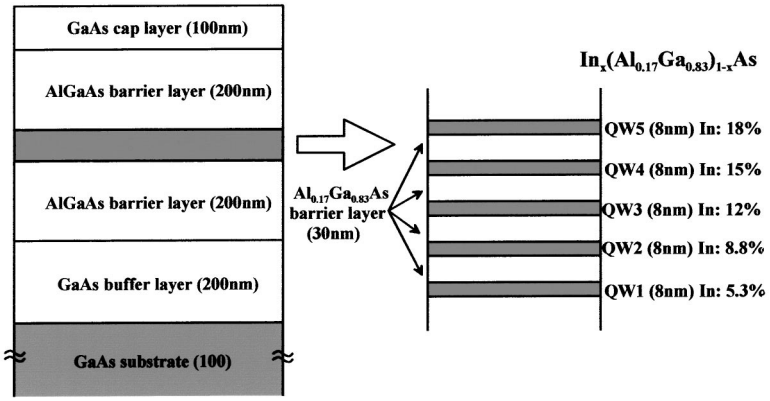

FIG. 2. Layered structure of step-graded staircase heterostructure consisting of strained $In_x(Al_{0.17}Ga_{0.83})_{1-x}As$ multiple quantum wells with similar well widths but five different In mole fractions ($x=5.3$, 8.8, 12, 15, and 18%, named QW 1, 2, 3, 4, and 5, respectively).

detrapped carriers will move in both directions with an equal probability and should be recaptured, resulting in the radiative recombination. However, if a neighboring deeper well exists, the carriers escaping from the well are captured by the deeper well, causing perpendicular unidirectional motion. Our experimental and theoretical studies of the PL dynamics directly provide evidence of the perpendicular flowing of photoexcited carriers and the capture by the deeper QW's.

The paper is organized as follows. In Sec. II, experimental details of our sample and the measurements are reported. In Sec. III A, the results of PL spectral characteristics as well as the PL dynamics in Sec. III B are described, and the calculated results of rate-equation analysis are presented and discussed in Sec. III C. Finally, conclusions are given in Sec. IV.

II. EXPERIMENT

The novel step-graded ladder heterostructure consisting of strained $In_x(Al_{0.17}Ga_{0.83})_{1-x}As$ quantum wells was grown at 530 °C on a GaAs(100) substrate by molecular beam epitaxy.[13] The schematic layered structure is shown in Fig. 2. In this sample, nominal widths of the five wells are all about 8 nm. But the In mole fractions (x values) in the $In_x(Al_{0.17}Ga_{0.83})_{1-x}As$ well layers are 5.3, 8.8, 12, 15, and 18% in QW 1, 2, 3, 4, and 5, respectively, of the heterostructure. The sequence of QW 1, 2, 3, 4, and 5 starts from the substrate side. These QW layers, which are electronically isolated by 30-nm-thick $Al_{0.17}Ga_{0.83}As$ barriers, are further sandwiched between 200-nm-thick $Al_{0.17}Ga_{0.83}As$ barriers. The growth is terminated by a 100-nm GaAs cap layer. The growth details of the nominally undoped sample were given and characterized previously.[13] The structural parameters (well width) determined were 8.0 nm (QW1), 7.9 nm (QW2), 7.7 nm (QW3), 7.5 nm (QW4), and 7.3 nm (QW5). Spectrally and temporally resolved PL transients were measured at 12–90 K in a closed-cycle He cryostat using a pulsed semiconductor laser with 50-ps pulses at 653 nm for weak excitation (average power of 1 μW) by a streak camera detection system (Hamamatsu C 4334-02) with 10-ps resolution, after being dispersed by a 32-cm monochromator (Jovan-Yubon HR320). We detected PL transients in a time window of 10 ns in a photon-counting mode.

III. RESULTS AND DISCUSSION

A. PL spectra

Figure 3 shows time-integrated PL spectra for the five different QW layers at several temperatures. The baseline of the PL intensity is vertically shifted for clear comparison. In the lowest spectrum measured at 12 K, five distinct PL peaks corresponding to QW 1, 2, 3, 4, and 5 are clearly observed as assigned in the figure in agreement with the previous result and analysis.[13,14] We note in Fig. 3 that their relative PL intensity changes in a complex manner. For example, the PL peak intensity of QW3 is higher than that of the lower-energy peak of QW4. At present we do not exactly know the origin of the different relative PL intensities, although we may point out a possibility of resonant capture processes causing the PL intensity difference between the different QW layers at 12 K.[15]

However, an interesting point that we would like to discuss here is that their relative PL peak intensity evolves significantly when the lattice temperature is increased up to 90 K. At first glance it appears they change in a complicated way. However, we note that there exists a clear trend of the variations. That is, as the temperature increases, the PL peaks decrease their relative intensities progressively from shorter-wavelength sides after increasing the signal amplitude in the intermediate temperature range. For example, the QW3 PL peak shows the highest intensity at 50 K and then decreases monotonically above 60 K. For QW4 the PL intensity is highest at 70 K and decreases at 90 K.

Previously we have measured the cw PL spectra as a function of temperature in order to study detailed changes of the relative PL intensities.[14] Plots of the cw PL intensities as a function of temperature for different quantum wells have previously been shown in Ref. 14 and are not repeated here. The results of a quantitative plot of the wavelength-integrated PL intensities indicate that there are some plateaus or even restorations of the PL signal in the temperature range that depends on the QW potential depth. We attribute these PL intensity variations due to the population changes of photogenerated carriers in the wells, since there are no reasons to enhance the radiative recombination rate at higher temperatures. These results mean that the photoexcited carriers directionally move from shallower (QW 1 and 2) to deeper QW's (QW 3, 4, and 5) via phonon-assisted thermal activation above the barrier band-edge state before being radiatively recombined in the wells, as schematically illustrated in Fig. 4.

The seeming difficulty to observe PL enhancement for QW5 above 80 K is easily explained by activation of the efficient nonradiative recombination processes at higher tem-

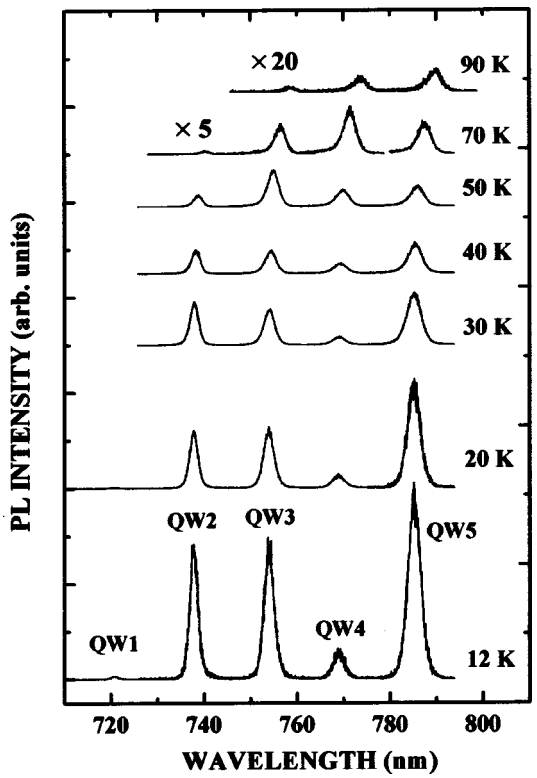

FIG. 3. Time-integrated PL spectra for lattice temperatures between 12 and 90 K.

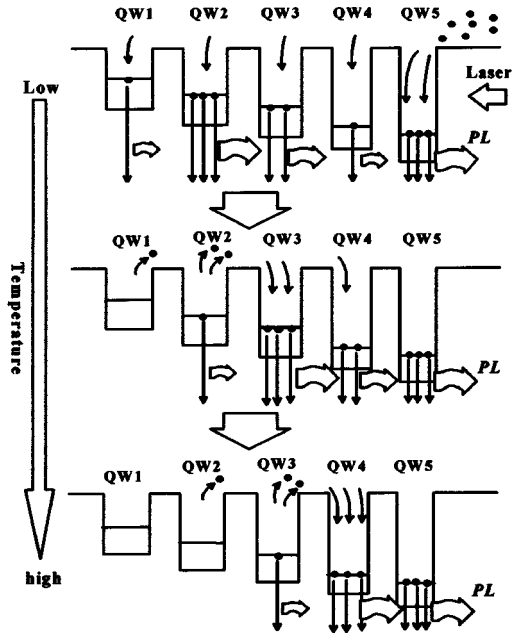

FIG. 4. Schematic potential diagram of five-step $In_x(Al_{0.17}Ga_{0.83})_{1-x}As$ multiple quantum wells and concept of carrier flow from shallower to deeper wells for different temperatures.

peratures, since a higher thermal activation energy is required for the deepest potential well. Here we stress the important concept, asymmetric thermionic emission, to elucidate these temperature-dependent variations of the PL signal. That is, the carriers populated in the wells are selectively activated and released from the shallower wells with increasing temperature. Once they are captured by the deeper well at a certain temperature, which depends on the well depth, they cannot go back to the shallower well. This will lead to the unidirectional transport of the carriers towards the lower potential side by the builtin field. This is because a higher thermal activation energy is required to escape from that particular deeper well at the given temperature, prohibiting the carriers moving back to the shallower well.

In order to justify the claimed carrier transport mechanism, we have made an analysis of thermal activation energies for the five quantum wells, as summarized in Table I. For this purpose, we estimate the potential depth for electron-hole pairs in each well from a difference in energy between the barrier band gap and the corresponding PL peak energy, ΔE_i $(=E_g-E_{\mathrm{PL}})$. A temperature at which the carriers can efficiently escape out of the particular well is estimated (from Fig. 3 of Ref. 14 and also from PL time behaviors, as discussed later) to determine the thermal activation energy (k_BT). Ratios of these parameters of ΔE_i listed in Table I coincide with those of the thermal activation energy at least for QW2, QW3, and QW4. This fact supports our argument for the mechanism of the phonon-assisted perpendicular carrier transport. These experimental findings indicate that unidirectional phonon-assisted transport of photoexcited carriers is actually occurring in this novel stepped QW heterostructure.

B. PL dynamics

Measurements of the PL dynamics directly provide evidence of the perpendicular flowing of photoexcited carriers and the capture by the deeper QW. Figure 5(a) shows wavelength-integrated PL transients at several temperatures as a function of time after the laser excitation pulse $(t=0\ \mathrm{ns})$ for the emission band of QW2 as well as those for the emission bands of QW3 and QW4 in Figs. 5(b) and 5(c), respectively. At 12 K the PL time behavior of QW3 shows the typical two-component exponential decays,[16] fast and slow, with an initial fast decay and a time constant of 0.46 ns due to the free heavy-hole excitons, which follows a slower decay of 2.9 ns attributable to the localized excitons, caused by the confinement potential fluctuations. Increasing the temperature from 12 to 40 K, on the other hand, the two-

TABLE I. Thermal activation energy and depth of potential well for electron-hole pairs. The values in parentheses for k_BT and T indicate the upper and lower bound from the estimation. The ratios are normalized for QW2.

Well number	Potential depth ΔE_i (meV)	Ratio	k_BT (meV)	Ratio	T (K)
QW1	38	0.49	($\leqslant$1.7)	$\leqslant$0.49	($\leqslant$20)
QW2	78	1.0	3.5	1.0	35
QW3	114	1.5	4.8	1.4	55
QW4	148	1.9	6.9	2.0	80
QW5	183	2.3	($\geqslant$7.8)	$\geqslant$2.5	($\geqslant$90)

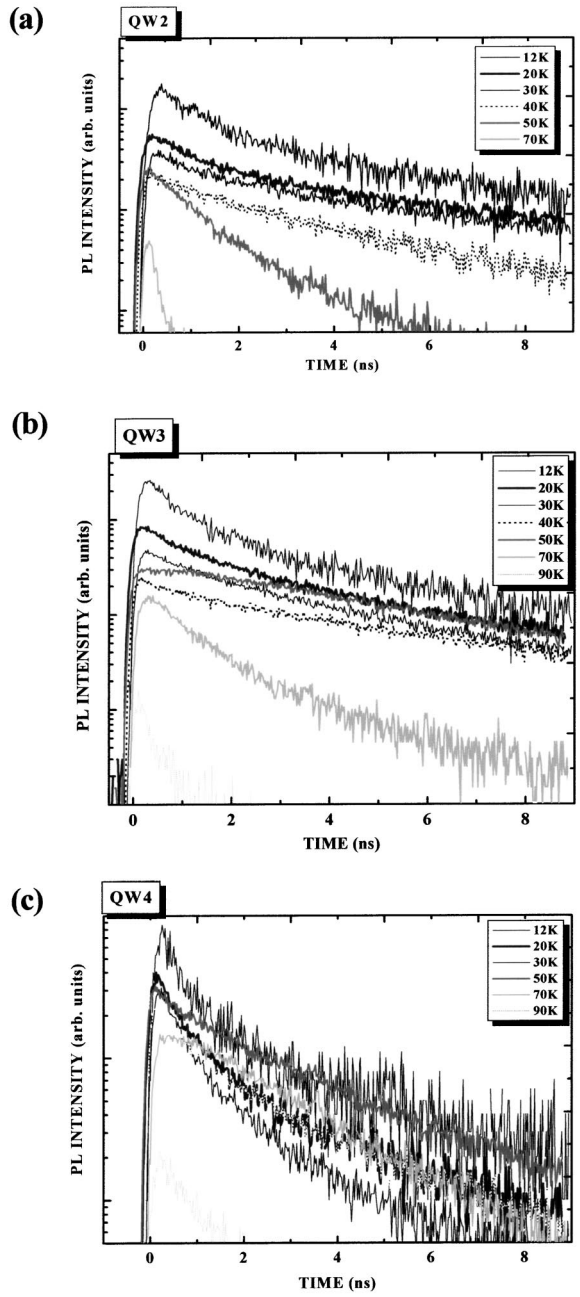

FIG. 5. Semilogarithmic plots of PL intensity for emission bands of (a) the QW2, (b) QW3, and (c) QW4 as a function of time at six or seven temperatures. Note that at 50 K the PL transient of QW3 in (b) shows a significant increase of the rise time and the intensity, while the PL decay at 70 K is faster, determined by the escape time of carriers to QW4. Also note at 50 K in (a) that the PL decay of QW2 is shortened by the carrier escape towards QW3. The laser excitation pulse is located at $t=0$ in the ordinate of this figure.

component PL decays merge into a single exponential time behavior with a longer time constant of 3.0 ns at 40 K for QW3 because of the thermal delocalization within the inhomogeneously broadened exciton band. In addition, the slower decays at higher temperatures accompany the PL intensity decrease. The increase of the PL decay time can easily be understood in terms of the temperature-dependent radiative recombination rate of free excitons in QW,[17] while the decrease of the PL intensity with temperature is ascribed to the thermal activation of nonradiative recombination centers. However, we stress here that a significant increase of the PL rise accompanying the drastic PL intensity enhancement is clearly observed for QW3 when the temperature is increased to 50 K in Fig. 5(b), for example. This recovery of the PL intensity and the appearance of PL rise are unique in this type of stepped QW sample and provide firm evidence for the carrier flow and capture processes assisted by phonon scattering.

At 50 K, we note that when the PL intensity of QW3 is significantly increased, a faster PL decay (quenching) of the neighboring shallow QW2 is observed in Fig. 5(a), which verifies the carrier escape from QW2 and the trapping into QW3. When the temperature is further increased to 70 K, the PL decay of QW3 becomes even faster with a time constant of 1.1 ns as seen in Fig. 5(b), revealing the transfer of carriers to the deeper neighboring QW4 where the transient PL intensity is enhanced [see Fig. 5(c)]. At 90 K, the PL intensity for QW3 is very quickly quenched by complete transferring to the deeper QW4. For the time behaviors of QW2 and QW4 shown in Figs. 5(a) and 5(c), respectively, basically similar characteristics are seen of the PL intensity increasing with the increased rise times and of the PL reductions accompanying the rapid decays, except for variances in temperature. These results of PL transients clearly and directly demonstrate the dynamical carrier flow and capture processes between the different QW layers. We note that the carrier motion is always directed from the shallower to the deeper well with the higher In mole fraction due to the built-in potential gradients.

In order to analyze the PL time behaviors, we have first made three-component exponential fitting to the PL transients with one rise time reflecting the carrier flow and two decay time constants, fast and slow for the free and localized excitons, respectively. The results of the representative fitting at 12 and 50 K are illustrated in Figs. 6(a) and 6(b), respectively, by solid curves for the five or four wells (QW1, QW2, QW3, QW4, and QW5) together with the experimental PL data, assuming the instrumental time response function. A good fitting is obtained for all the wells. The fitting time constants thus determined are plotted in Figs. 7(a) and 7(b), for the fast decay and the rise times, as a function of temperature. When the temperature is slightly increased to 30 K, the decay times generally increase as a result of reduced thermal population at the exciton states where the radiative recombination is possible near $K \approx 0$.[17] These increases of the PL decay times are, however, interrupted with further increases of the temperature (for example, at 70 K for the case of QW3). That is, the PL lifetime then is basically determined by the carrier escape time (thermal detrapping). Therefore, in the case of QW3 at 70 K, the photoexcited carriers are very efficiently transferred into the neighboring deeper QW4 by phonon scattering. The observed enhancement of the PL rise time at 70 K for QW4 in Fig. 7(b) is consistently explained by the carrier flow into the QW4 layer from QW3. Similar enhancement of the rise time at 50 K for QW3 in Fig. 7(b) coincides with a drastic decrease of the

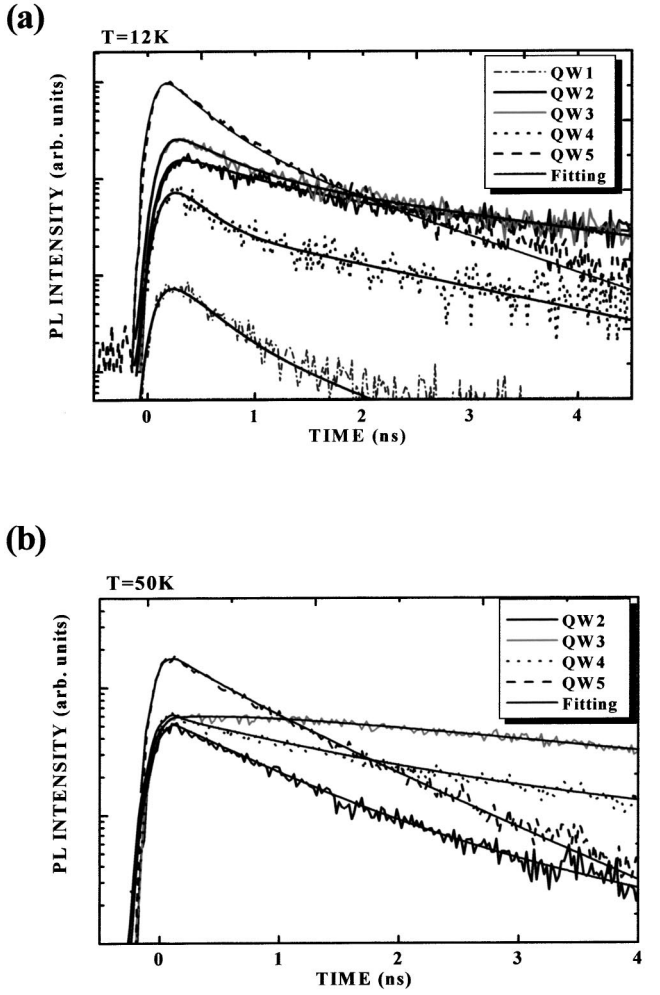

FIG. 6. Three-component (one rise and two decays) exponential fitting (smooth solid curves) of the PL transients together with the experimental data at (a) 12 K and at (b) 50 K.

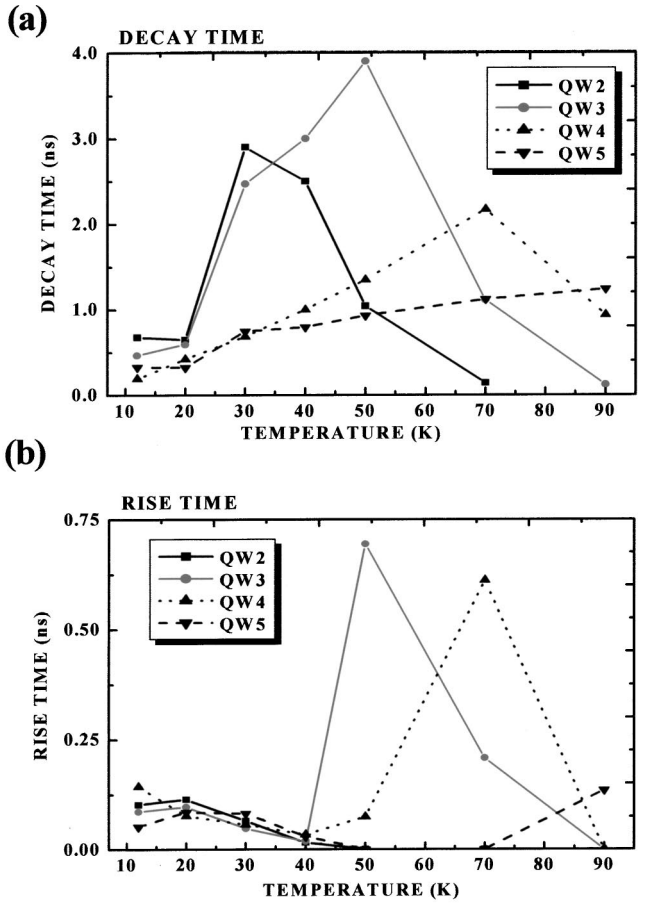

FIG. 7. (a) Decay and (b) rise times deduced from the three-component exponential fitting of the PL transients for QW2, QW3, QW4, and QW5 as a function of temperature.

decay time of QW2 in Fig. 7(a). Therefore these results mean that the photoexcited carriers are moving from QW2 (QW3) to QW3 (QW4) at 50 K (70 K) along the growth direction as a result of asymmetric thermionic emssions. Apart from minor scatterings of the estimated characteristic time constants, overall features of the temperature-dependent PL transients are thus rigorously explained by successive carrier flowing from the shallower to the deeper wells with increase of temperature. We note once again that this type of phonon-assisted carrier transport is driven totally by the builtin potential field in the tailored quantum heterostructure.

C. Rate-equation analysis

Our experimental finding of the PL dynamics can be better understood by simulating the PL transients based on a rate-equation analysis. For this purpose, we have made numerical calculations of the five-component rate equation for the exciton or electron-hole pair occupation number N_i ($i=1$, 2, 3, 4, and 5) in QW1, QW2, QW3, QW4, and QW5, respectively. Assuming ratios of the carrier generation rate r_i in QWi by direct laser excitation [the generation function is defined as $G(t)$], these five rate equations are given by

$$\frac{dN_1}{dt}=r_1G(t)-\frac{N_1}{\tau_{R1}}-\frac{N_1}{\tau_{\mathrm{NR}}}-\frac{N_1}{\tau_{12}}, \tag{1}$$

$$\frac{dN_2}{dt}=r_2G(t)+\frac{N_1}{\tau_{12}}-\frac{N_2}{\tau_{R2}}-\frac{N_2}{\tau_{\mathrm{NR}}}-\frac{N_2}{\tau_{23}}, \tag{2}$$

$$\frac{dN_3}{dt}=r_3G(t)+\frac{N_2}{\tau_{23}}-\frac{N_3}{\tau_{R3}}-\frac{N_3}{\tau_{\mathrm{NR}}}-\frac{N_3}{\tau_{34}}, \tag{3}$$

$$\frac{dN_4}{dt}=r_4G(t)+\frac{N_3}{\tau_{34}}-\frac{N_4}{\tau_{R4}}-\frac{N_4}{\tau_{\mathrm{NR}}}-\frac{N_4}{\tau_{45}}, \tag{4}$$

$$\frac{dN_5}{dt}=r_5G(t)+\frac{N_4}{\tau_{45}}-\frac{N_5}{\tau_{R5}}-\frac{N_5}{\tau_{\mathrm{NR}}}. \tag{5}$$

For the calculations, we take into account the radiative (τ_{Ri}) and nonradiative (τ_{NR}) recombination times and the transfer time τ_{ij} from the ith well to the neighboring jth well at the lower potential side. It is worth noting here that we only need to use a single nonradiative lifetime (τ_{NR}) due to the common $Al_{0.17}Ga_{0.83}As$ barriers at a fixed lattice temperature, while the five radiative recombination times (τ_{Ri}) that are approximately linearly dependent on temperature[17] are assumed. We treat these characteristic time constants as ad-

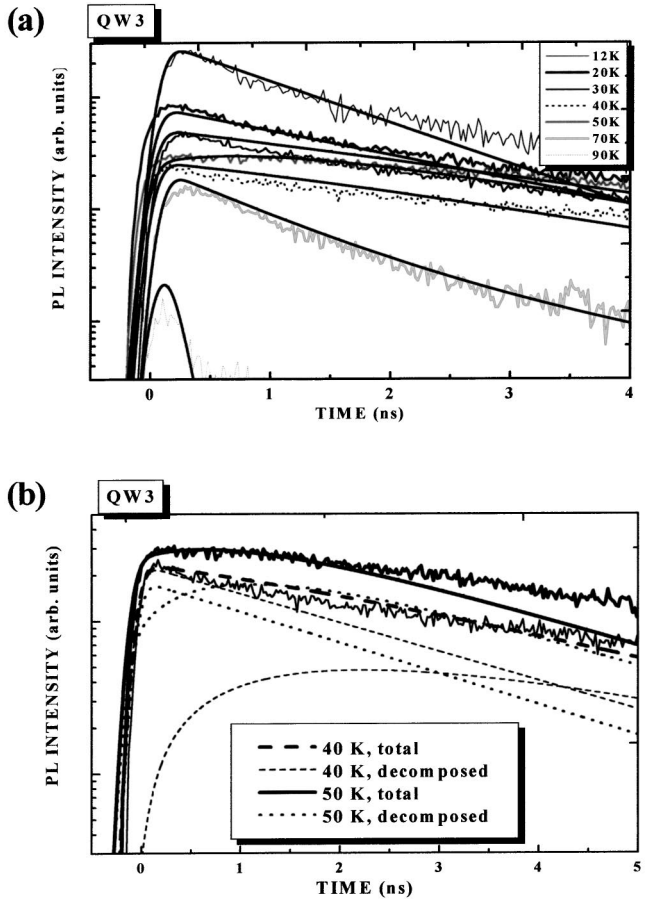

FIG. 8. Simulated PL transients (smooth solid curves) together with the experimental data for QW3 in (a) at 12, 20, 30, 40, 50, 70, and 90 K. In (b), the experimental PL transients and the simulated results (by smooth solid and dashed curves) are plotted for QW3. Here the simulated PL transients are also decomposed into the two components, by dotted curves at 50 K and by dashed curves at 40 K, corresponding to the carrier generation by laser excitation (with fast rise) and the phonon-assisted transfer from the neighboring shallower well (with slow rise).

justable parameters, which are all temperature dependent. For calculational simplicity, we assume that the carrier transfer beyond the nearest-neighbor wells can be neglected. We also assume that the carrier generation by laser excitation in each well is fast enough, neglecting the initial energy relaxation processes from the barrier state. Using the transient population $N_i(t)$ numerically calculated, the PL transient, $I^i_{\mathrm{PL}}(t)$ is determined by the equation $I^i_{\mathrm{PL}}(t)=N_i(t)/\tau_{Ri}$. Further details of the calculations will be reported elsewhere. These procedures allow us to almost perfectly fit the PL transients for the five emission bands. Simulation results are plotted in Fig. 8(a) for QW3 at temperatures of 12, 20, 30, 40, 50, 70, and 90 K. Both the PL intensity and time behaviors are all well reproduced in Fig. 8(a), assuming an almost linear temperature dependence of τ_{Ri} and reduced $\tau_{\mathrm{NR}\,i}$ values with temperature.

An important issue from this simulation is, as shown by dotted (at 50 K) and dashed (at 40 K) curves in Fig. 8(b), that the two types of the carrier supply process for the transient PL can be decomposed by direct laser excitation and by phonon-assisted transfer. At 40 K, the PL transient contribution by laser excitation is much stronger, while the other component with a slow rise due to the transfer from QW2 shows only a minor contribution. Therefore, the former contribution almost determines the total PL transient, shown by a thick dashed curve. However, it is clear that at 50 K, most of the PL transient signal, especially after 0.5 ns, comes from the carrier transfer from the neighboring well (QW2). This efficient phonon-assisted carrier transport from the neighboring shallower well is responsible for the enhanced PL transient at 50 K with the appearance of the rise time. On the other hand, we note that the decomposed PL transient due to the direct laser excitation at 50 K is always lower than that at 40 K because of the decreased nonradiative lifetime (decreased internal quantum efficiency). These results of the decomposed PL transients show that the enhanced, nonexponential PL time behavior of QW's (for example, at 50 K for the case of QW3) is explained by the additional carrier supply by the neighboring well (QW2) in terms of the directional transport of carriers assisted by phonon scattering.

IV. CONCLUSIONS

The temperature dependence of transient photoluminescence properties has been investigated by time-resolved photoluminescence experiments and a rate-equation analysis in a novel step-graded staircase heterostructure consisting of strained $\mathrm{In}_x(\mathrm{Al}_{0.17}\mathrm{Ga}_{0.83})_{1-x}\mathrm{As}$ multiple quantum wells with similar widths but five different x values. It is found that the PL dynamics of the different quantum wells drastically evolve with the lattice temperature. The results of transient PL variations with temperature indicate that the photoexcited carriers directionally move from the shallower to the deeper quantum wells by phonon-assisted transfer via activation to the barrier band-edge state. These findings suggest that a design of stepped heterostructures with builtin potential gradients can be used to tailor directional motion of carriers in quantum heterostructures.

ACKNOWLEDGMENTS

The authors would like to thank A. Satake for his useful comments on the rate-equation analysis. One of the authors (K.F.) would like to thank the Paul-Drude Institute for Solid State Electronics in Berlin, especially K. H. Ploog and H. T. Grahn, for their kind hospitality.

*Author to whom correspondence should be addressed. Electronic address: fujiwara@ele.kyutech.ac.jp

[1] R. H. Fowler and L. Nordheim, Proc. R. Soc. London, Ser. A **119**, 173 (1928).

[2] R. Tsu and G. Döhler, Phys. Rev. B **12**, 680 (1975).

[3] F. Capasso, K. Mohammed, and A. Y. Cho, Appl. Phys. Lett. **48**, 478 (1986); IEEE J. Quantum Electron. **QE-22**, 1853 (1988).

[4] L. L. Chang, E. E. Mendez, and C. Tejedor, *Resonant Tunneling in Semiconductors* (Plenum, New York, 1992).

[5] B. Deveaud, J. Shah, T. C. Damen, B. Lambert, and A. Regreny,

Phys. Rev. Lett. **58**, 2582 (1987).
[6] B. Deveaud, J. Shah, T. C. Damen, B. Lambert, A. Chomette, and A. Regreny, IEEE J. Quantum Electron. **QE-24**, 1641 (1988).
[7] L. Esaki and R. Tsu, IBM J. Res. Dev. **14**, 61 (1970).
[8] H. Krömer, Rev. Mod. Phys. **73**, 783 (2001).
[9] *Semiconductor Superlattices: Growth and Electronic Properties*, edited by H. T. Grahn (World Scientific, Singapore, 1995).
[10] J. Faist, F. Capasso, D. L. Sivco, C. Sirtori, A. L. Hutchinson, and A. Y. Cho, Science (Washington, DC, U.S.) **264**, 553 (1994).
[11] H. Schneider, C. Schönbei, K. Schwarz, and M. Walter, Physica E (Amsterdam) **2**, 28 (1998).
[12] K. Fujiwara, N. Tsukada, T. Nakayama, and A. Nakamura, Phys. Rev. B **40**, 1096 (1989).
[13] J. R. Jensen, J. M. Hvam, and W. Langbein, J. Appl. Phys. **86**, 2584 (1999).
[14] S. Machida, M. Matsuo, K. Fujiwara, J. R. Jensen, and J. M. Hvam, Physica E (Amsterdam) **13**, 182 (2002).
[15] A. Fujiwara, Y. Takahashi, S. Fukatsu, Y. Shiraki, and R. Ito, Phys. Rev. B **51**, 2291 (1995).
[16] K. Fujiwara, H. Katahama, K. Kanamoto, R. Cingolani, and K. Ploog, Phys. Rev. B **43**, 13 978 (1991).
[17] J. Feldmann, G. Peter, E. O. Göbel, P. Dowson, K. Moore, C. Foxon, and R. J. Elliott, Phys. Rev. Lett. **59**, 2337 (1987).